



Tree demographics and soil charcoal evidence of fire disturbances in an inaccessible forest atop the Mount Lico inselberg, Mozambique

Courtney Mustaphi, Colin; Platts, Philip J.; Willcock, Simon; Timberlake, Jonathan; Osborne, Jo; Matimele, Hermenegildo; Osgood, Hanniah; Muiruri, Veronica; Gehrels, Maria; Bayliss, Julian; Marchant, Robert

Plants, People, Planet

Accepted/In press: 03/09/2024

Peer reviewed version

[Cyswllt i'r cyhoeddiad / Link to publication](#)

Dyfyniad o'r fersiwn a gyhoeddwyd / Citation for published version (APA):

Courtney Mustaphi, C., Platts, P. J., Willcock, S., Timberlake, J., Osborne, J., Matimele, H., Osgood, H., Muiruri, V., Gehrels, M., Bayliss, J., & Marchant, R. (in press). Tree demographics and soil charcoal evidence of fire disturbances in an inaccessible forest atop the Mount Lico inselberg, Mozambique. *Plants, People, Planet*.

Hawliau Cyffredinol / General rights

Copyright and moral rights for the publications made accessible in the public portal are retained by the authors and/or other copyright owners and it is a condition of accessing publications that users recognise and abide by the legal requirements associated with these rights.

- Users may download and print one copy of any publication from the public portal for the purpose of private study or research.
- You may not further distribute the material or use it for any profit-making activity or commercial gain
- You may freely distribute the URL identifying the publication in the public portal ?

Take down policy

If you believe that this document breaches copyright please contact us providing details, and we will remove access to the work immediately and investigate your claim.

Supporting Information

Table S1. AMS Radiocarbon date determinations.

Table S2. Charcoal morphotypes and entrainability index.

Figure S1. Soil accumulation rate estimates.

Figure S2. Theoretical entrainment indices and transport distance of charcoal morphotypes.

Supporting Information

Table S1. AMS Radiocarbon date determinations.

Laboratory code	Depth (cm)	p MC (%)	Radiocarbon age (^{14}C yr BP)	Calibrated 2σ range (cal yr BP)	Median calibrated age (cal yr BP)
D-AMS029604	39–40	79.76 \pm 0.38	1817 \pm 38	1587–1750	1682 \pm 82
D-AMS029605	75–76	67.72 \pm 0.27	3131 \pm 32	3183–3387	3295 \pm 102
D-AMS029606	201–202	43.94 \pm 0.24	6606 \pm 44	7421–7571	7475 \pm 75

Table S1. Results of AMS radiocarbon dating of soil organic matter. Uncalibrated ^{14}C ages have not been rounded (Stuiver and Polach, 1977). Radiocarbon ages were calibrated with the SHCal20 curve (Hogg et al., 2020) and have not been rounded. The age determinations were used to estimate soil accumulation rates and to calculate charcoal accumulation rates (see Figures 3, 6 and 7). Acronyms: p MC, percent Modern Carbon; cal yr BP, calibrated years Before Present (1950 Common Era).

REFERENCES FOR TABLE S1

Hogg, A.G., Heaton, T.J., Hua, Q., et al. (2020) SHCal20 Southern Hemisphere calibration, 0–55,000 years cal BP. *Radiocarbon*, 62(4), 759–778.

Stuiver, M., & Polach, H.A. (1977). Discussion reporting of ^{14}C data. *Radiocarbon*, 19(3), 355–363.

Supporting Information

Figure S1. Soil accumulation rate estimates.

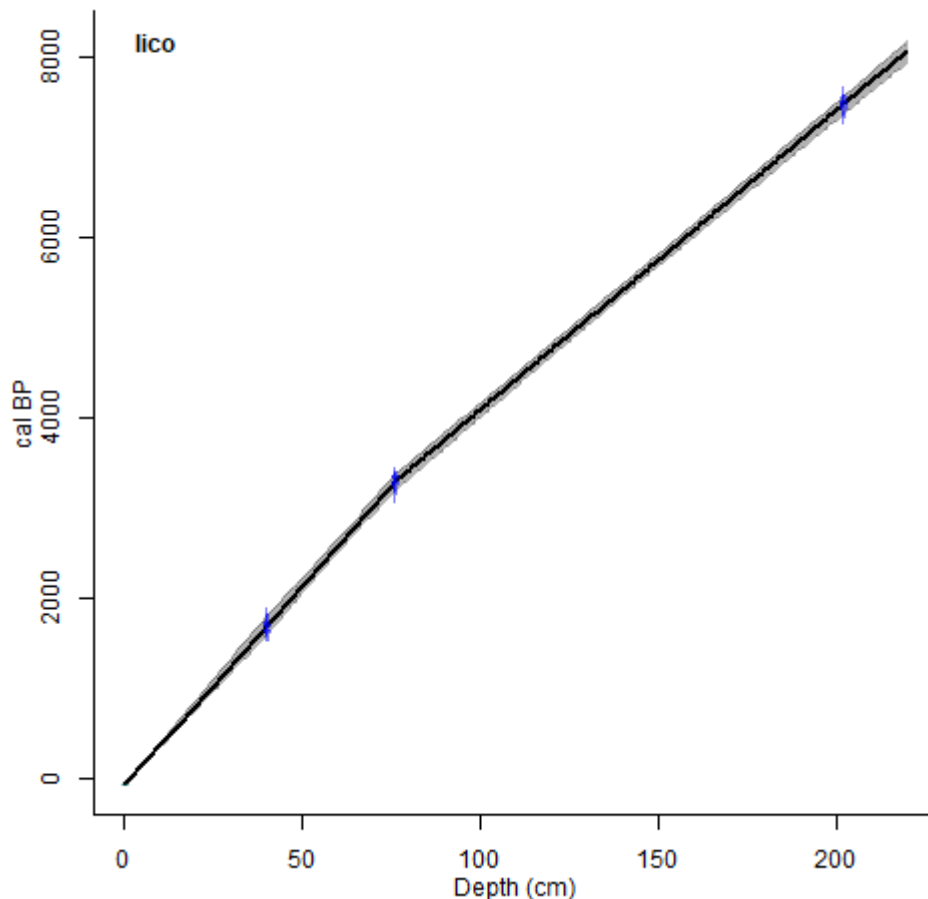


FIGURE S1. Estimates of soil accumulation rates based on three radiocarbon date geochronological determinations in the Mount Lico soil pit. Linear interpolated age-depth model of three AMS radiocarbon determinations from the Mount Lico soil pit calibrated with the SHCal20 calibration curve (Hogg et al., 2020) generated with the R package ‘clam’ (Blaauw, 2010) and replotted in Figure 3.

REFERENCES FOR FIGURE S1

Blaauw, M. (2010) Methods and code for ‘classical’ age-modelling of radiocarbon sequences. *Quaternary Geochronology*, 5(5), 512–518.

Hogg, A.G., Heaton, T.J., Hua, Q., et al. (2020) SHCal20 Southern Hemisphere calibration, 0–55,000 years cal BP. *Radiocarbon*, 62(4), 759–778.

Supporting Information

Table S2. Charcoal morphotypes and entrainability index.

Shape	Type	Description	Features	Dimensionality	Entrainability index >250µm observed (1=easily, to 5=resistant)	
Polygonal	A1	Irregular, subangular polygon	Solid with parallel striations	2D	2	yes
	A2	Irregular, subangular polygon	Solid with conspicuous stomata holes	2D	1	
	A3	Irregular, subangular polygon	Solid and featureless	2D	2	
	A4	Irregular, subangular polygon	Structured reticulate mesh	2D	1	
	A1a	Irregular, subangular polyhedron	Solid with parallel striations	3D	3	yes
	A3a	Irregular, subangular polyhedron	Solid and featureless	3D	3	yes
Blocky	B2	Rectangular	Solid with parallel striations	2D	3	
	B3	Rectangular	Solid and featureless	2D	3	
	B4	Rectangular	Solid with conspicuous stomata holes	2D	1	
	B5	Rectangular	Structured reticulate mesh	2D	1	
	B2.1a	Cubic	Solid with parallel striations	3D	5	
	B5.1	Rectangular	Structured reticulate mesh with venation	2D	1	
	B2a	Rectangular prism	Solid with parallel striations	3D	5	yes
	B3a	Cubic	Solid and featureless	3D	5	
	B5a	Rectangular prism	Structured reticulate mesh, often at least partially filled	3D	4	
	Elongate	D1	Long, very thin and straight	Solid and featureless	2D	1
D2		Long, thin and straight	Solid and featureless	2D	2	
D4		Long, thin and straight	Solid with parallel striations	2D	2	
D5		Long, thin, hollow cylindrical	Solid with parallel striations	3D	1	
D5.1		Long, thin, outer hemicylinder	Solid with parallel striations	3D	1	
D4a		Long, thin rectangular prism	Solid with striations	3D	4	yes
D5a		Long, thin, solid cylindrical	Solid with parallel striations	3D	2	
D6.1a		Long, thin, hollow cylindrical	Structured reticulate mesh	3D	3	
Other	E	Slightly curved irregular prism	Resembled charred non-woody plant part	3D	5	yes

TABLE S2. Descriptions of charcoal morphotypes >125 µm in the Mount Lico soil profile that accompany the idealised forms presented in Figure 5. The apparent dimensionality at 10–40× magnifications: charcoal that appeared thin in the optical z-axis and tends to lie flat in the Petri dish and nearly impossible to lie stationary when stood on the thin axes was classed as 2D, and 3D charcoal had a visually obvious z-axis thickness and could lie stationary at the bottom of Petri dish when manually probed and rotated. The final column lists if charcoal morphotypes observed >250 µm at any depth in the soil profile regardless of fragment morphotype (Figure 6). Type E superficially resembled a fragment of charred succulent xerophyte leaf.

Supporting Information

Figure S2. Theoretical entrainment indices and transport distance of charcoal morphotypes.

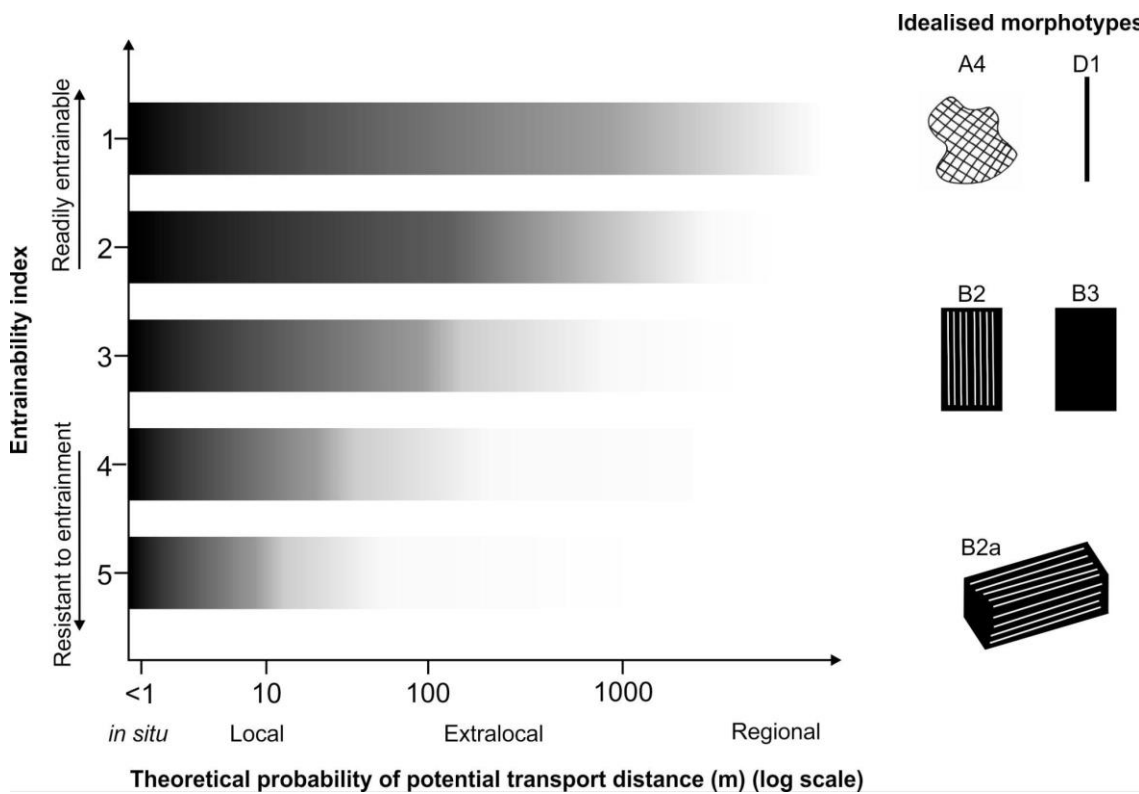


Figure S2. Conceptual diagram of potential theoretical transport distances (x-axis log scale) to final deposition for entrainability indices (discrete classes 1–5, y-axis) based on charcoal morphotypes (irrespective of charcoal size) produced at a point source fire. All morphotypes have the potential to be produced and deposited in situ, local to the fire, or transported by convection and advection. Readily entrainable charcoal morphotypes have a higher probability to be transported to extralocal and regional scales before final deposition, relative to charcoal morphotypes that have a higher inertia to entrainment and that would require much more energy to sustain transport beyond local distances.